Probing the darkness : the link between baryons and dark matter

Velliscig, M.

Author: Velliscig, Marco
Title: Probing the darkness : the link between baryons and dark matter
Issue Date: 2015-11-11

1

Introduction

1.1 Numerical simulations in astrophysics

In a field of research such as astrophysics that studies objects beyond our reach, the role of direct experimentation is very limited. Simulations often take the role of experimentation in astrophysics, and allow us to conduct trials while modifying parameters in a manner similar to experiments. For an experiment to be successful, it needs to validate a hypothesis by confronting the predictions with real data. In the same way, simulations need to be compared against observations to understand to which degree they can reproduce the observables in the Universe.

If we were able to correctly simulate every process that has astrophysical significance, we could create a simulation that reproduces every possible observable, and we would be confident in our understanding of the physics governing our Universe. Of course, such a scenario is out of our reach and will likely remain so for many years. In the meantime, simulations can be used to guide the interpretation of observations, and for the design of new observational campaigns and instruments.

1.1.1 Dark matter-only simulations

Even the most basic cosmological simulations need to include the most important process for astrophysics: gravity. For this reason, N-body simulations were historically the first attempt to simulate our Universe. In N-body simulations all of the mass in the universe is only able to interact gravitationally. This approach, even if simplistic, has proven to be very successful for predictions of the large-scale distribution of matter, the halo abundance in a unit volume (the halo mass function), and the matter density profiles of haloes.

Moreover, even in recent years, only with dark matter simulations is it possible to simulate large volumes of the Universe with high resolution, or many realisations of small volumes with different cosmological parameters. For this reason, dark matter haloes in N-body simulation are often 'painted' with galaxies following simple prescriptions often calibrated to reproduce observables, an approach called semi-analytical modelling.

Even in this basic approach, some assumptions need to be made. For example, the particle mass of the simulated dark matter is many orders of magnitude greater than any theoretical expectation. This simplification is necessary because, even when neglecting hydrodynamics, the number of calculations required to evolve a system scales with the number of particles. Therefore, to keep the computational times reasonable the number of particles must be limited.

For a complete review on the topic please see Frenk & White (2012).

1.1.2 Hydrodynamical simulations

The next ingredient that needs to be included in simulations is the physics of the gas. However, before the processes that regulate the physical state of the gas can be included, the gas itself should be modelled to follow the basic hydrodynamical equations. There are usually two different approaches to solve the hydrodynamical equations in simulations: the Eulerian approach and the Lagrangian approach. In the Eulerian approach, the cosmological volume is divided in small, discrete sub volumes, inside which the properties of the gas are simulated. In order to achieve higher resolutions, these volumes are subdivided in smaller parts where needed. In the Lagrangian approach, the mass of the gas is divided into particles that can interact with each other, and these are followed in time. The Lagrangian approach offers the advantage that the mass resolution is fixed and in turn the most dense parts of the Universe are naturally simulated with more particles. In this thesis, we use Lagrangian simulations realized using a technique known as smooth particle hydrodynamics (SPH, for a recent review see Springel 2010).

Baryonic physics in simulations

The physical state of the gas can be influenced by many processes, most of which are related to star formation and evolution. Stars produce radiation which can heat the gas and exert radiation pressure. Moreover the radiation from stars can change the ionisation balance of the gas and hence the rate at which it cools. Massive stars explode as supernovae (SNe) which can drive small-scale turbulence in the gas and produce large-scale outflows, a process referred to as SN feedback. Stars also produce heavy elements and dust which change the rate at which gas cools. The effect of star formation on the gas can also influence the star formation itself, making very difficult to predict it without self-consistently simulating both the star formation and the physical processes that alter the physical state of the gas. A similar role is played by the formation and evolution of supermassive black holes (SMBHs). Gas accretion onto SMBHs in the centres of galaxies can also result in radiative, thermal and mechanical feedback.

Many of the processes that are included in hydrodynamical simulations such as radiative cooling, photo-heating, star formation, metal enrichment are happening on scales that are orders of magnitude smaller than the scales which can be reasonably resolved in simulations. For this reason, such processes are usually taken into account using so called ‘subgrid’ models. As in the case of N-body simulations, the gas is simulated in parcels that represent millions of solar masses of gas. With current computational capabilities it would be unthinkable to model gas at the atomic or molecular level. Therefore, we make use of models that translate molecular processes to much larger mass scales.

The simultaneous simulation of all these physical processes has a large impact on the computational cost of the simulations. Therefore, hydrodynamical simulations are often carried out in smaller boxes or with lower resolution than their N-body counterparts. On the other hand, hydrodynamical simulations allow one to self-consistently simulate the baryonic physics that ultimately produces the luminous matter that we see and study in our Universe.

OWLS and EAGLE hydrodynamical cosmological simulations

The analysis performed in this thesis is mostly based on two sets of hydrodynamical cosmological simulations: OWLS and EAGLE. OWLS stands for the OverWhelmingly Large Simulations project (OWLS; Schaye et al. 2010) and it consists of a suite of cosmological simulations with varying simulation volume and resolutions. OWLS is well-suited to study baryonic effects as it consists of a wide range of models that were run from identical initial conditions, but employing a wide variety of recipes for the uncertain baryonic processes. OWLS also includes a N-body only version that allow us to directly compare with the results obtained with the inclusion of baryon physics. In order to extend the mass range that can be studied, we often employed a larger volume, lower resolution versions of a subset of the OWLS models (called cosmo-OWLS; see Le Brun et al. 2014; McCarthy et al. 2014).

EAGLE stands for Evolution and Assembly of GaLaxies and their Environments (Schaye et al. 2015; Crain et al. 2015). A new approach adopted by EAGLE is to calibrate the feedback efficiency to reproduce the observed number of galaxies per unit volume (the galaxy stellar mass function), since most of the radiative losses are due to unresolved physics and so can not be simulated by first principles. This results in a successful mapping between the stellar mass and the halo mass, a task that has proven to be difficult to achieve by simulations.

Combining OWLS and EAGLE provides us the unique opportunity to span a wide range of masses and spatial scales. Moreover, we have access to sufficient cosmological volume and resolution to study the reliability and the applicability of our results to the different astrophysical questions addressed in this thesis.

The interaction between baryons and dark matter

For many purposes it is a reasonable approximation to assume that the effect of baryon physics on the matter distribution is negligible. This approximation is valid for instance, in the intergalactic medium and on the outskirts of galaxy clusters where the gas has a long cooling time and approximately traces the dark matter. However, it is clear that on small scales and in lower mass haloes, where the gas condenses to high densities due to cooling, baryonic processes such as galactic winds can have important effects on the matter distribution. Moreover, the distribution of the dark matter will itself adjust to the resulting change in the gravitational potential.

In **Chapter 2** we examine the effect of baryon physics on the masses and profiles of haloes and on the halo mass function as inferred by hydrodynamical simulations. The study of how the inclusion of baryonic physics can alter the properties of cosmological haloes represents the first step in exploring the connection between baryons and their host haloes.

1.2 Gravitational lensing

Gravitational lensing (GL) represents a powerful tool to measure what cannot be seen directly but what is an essential part of the mass of the Universe: the dark matter.

Here we give an introduction to gravitational lensing, focusing mostly on weak lensing and on the aspects and applications most relevant for this thesis. We refer to Bartelmann & Schneider (2001) for a more comprehensive review of the vast field of weak gravitational lensing.

Gravitational lensing is the effect of the gravitational potential on the light path of photons travelling trough it. “Gravitational" refers to the fact that this effect depend solely on the gravitational potential, making it insensitive to the dynamical state or the type of matter that generates it. “Lensing" stands for the fact that this effect acts on the light in the same way as a optical lens does. The light travelling from a distant source is lensed by the intervening gravitational field, and the image on the sky appears to be displaced, magnified and distorted by the interaction of the photons with the gravitational potential. Gravitational lensing can be exploited to measure different properties of the matter in the Universe, some of which we are going to briefly review in the next sections.

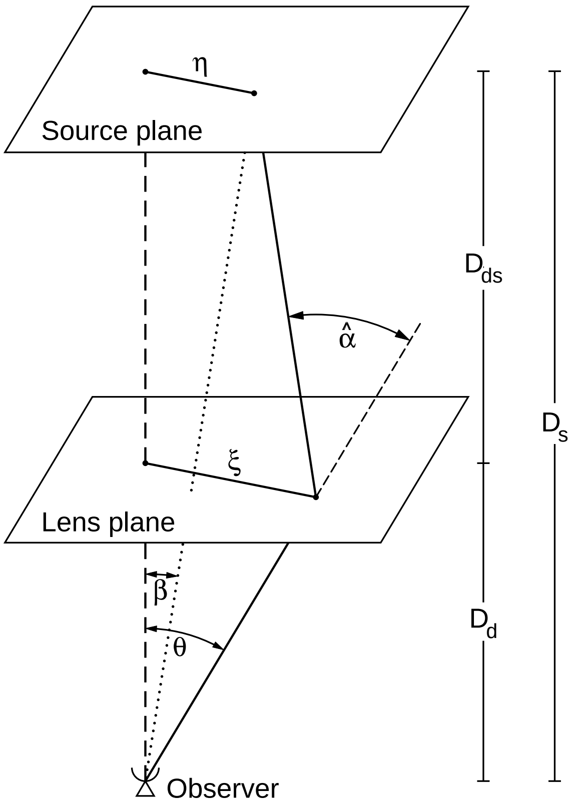

Figure 1.1: Basic schematics of a lensed light ray (from Bartelmann & Schneider 2001).

1.2.1 Single lens

The basic concept of GL can be reviewed by analysing the effect of a single lens on the light path of a single light ray. The thin lens approximation is commonly applied, which is valid if the mass distribution is extended over a region that is small compared to the distance between source and lens, and between lens and observer. Using this approximation, we can assume that the total mass of the lens is lying in a plane, and that a light ray passing through will be deflected once and instantaneously. The light rays, which are smoothly curved in the neighbourhood of the lens, can therefore be replaced by two straight rays that change their direction only in the plane of the lens. In Fig. 1.1 we show a schematic representation of a lens system. The source of photons lies in the source plane at the position η and at the angular diameter distance $D_{\rm s}$ (or redshift $z_{\rm s}$) away from the observer. The lens lies in the lens plane at a distance $D_{\rm l}$ from the observer and $D_{\rm ls}$ from the source. In the case where the lens is not present, the light ray emitted from the source would be observed at the angle β. The effect of the lens is to deflect the light ray, at the impact parameter ξ, by an angle of $\hat{\alpha}$. This results in the light ray being seen by the observer at an angle θ. The deflection is then:

$$\vec{\hat{\alpha}} = \frac{4GM}{c^2 \, \vec{\xi}} \ , \tag{1.1}$$

where M is the mass of the lens, G is the gravitational constant and $\vec{\xi}$ is the impact parameter vector. Therefore, the deflection angle not only depends on the mass of the lens but also on the impact parameter.

From this equation it is possible to understand the basic effect of gravitational lensing. Due to the presence of the lens, more light rays are converged towards the observer than otherwise, resulting in a magnification of the source. Since the deflection angle depends on the impact parameter, light rays that are passing at different distances from the source are deflected at different angles, producing a distortion in the original shape of the source. In extreme cases when the source is perfectly aligned with the lens this will produce a circular image, known as Einstein ring.

The angular diameter distance is defined as the ratio between the projected separation and the angle under which it is seen in the sky, and so $\vec{\theta} = \vec{\xi}/D_{\rm l}$ and $\vec{\beta} = \vec{\eta}/D_{\rm s}$. The projected separation of the source depends on the the line of sight η, the impact parameter and the deflection angle as:

$$\vec{\eta} = \frac{D_{\rm s}}{D_{\rm l}} \vec{\xi} - D_{\rm ls} \vec{\hat{\alpha}}(\vec{\xi}) \ . \tag{1.2}$$

By using the definition of $\vec{\beta}$ and $\vec{\theta}$, this can be rewritten as the commonly known lens equation:

$$\vec{\beta} = \vec{\theta} - \frac{D_{\rm ls}}{D_{\rm s}} \vec{\hat{\alpha}}(D_{\rm l}\vec{\theta}) \equiv \vec{\theta} - \vec{\alpha}(\vec{\theta}) \ , \tag{1.3}$$

where $\vec{\alpha}(\vec{\theta})$ is the deflection angle scaled by the distances from the lens and observer and the lens and source. The convergence parameter κ is defined as:

$$\kappa(\vec{\theta}) = \frac{\Sigma(D_{\rm d}\vec{\theta})}{\Sigma_{\rm cr}} \quad \text{with} \quad \Sigma_{\rm cr} = \frac{c^2}{4\pi G} \frac{D_{\rm s}}{D_{\rm d} \, D_{\rm ds}} \ , \tag{1.4}$$

where $\Sigma_{\rm cr}$ is the critical surface mass density (which depends on the redshifts of source and lens). The lens equation can have more than one $\vec{\theta}$ for a fixed $\vec{\beta}$ if the convergence parameter $\kappa > 1$, in which case the lensing is *strong*. In this thesis we focus on weak lensing for which $\kappa \ll 1$.

1.2.2 Statistical weak lensing

The net effect of gravitational lensing is, through the deflection of light rays, a re-mapping of the image of a source on to the plane of the observer. If the source image is small compared to the scale on which the properties of the lens change, the mapping can be described by the deflection matrix. The deflection matrix maps the unlensed surface brightness of the source $I(x, y)$ to the observed one $I'(x', y')$, as:

$$\begin{bmatrix} x' \\ y' \end{bmatrix} = (1-\kappa) \begin{bmatrix} 1-g_1 & -g_2 \\ -g_2 & 1+g_1 \end{bmatrix} \begin{bmatrix} x \\ y \end{bmatrix}, \tag{1.5}$$

where (x, y) are the true coordinates, (x', y') are the distorted ones, and κ is the convergence. The reduced shear g is related to the shear by $g_1, g_2 = (\gamma_1, \gamma_2)/(1-\kappa)$ and in the case of weak lensing, where $\kappa \ll 1$, $\gamma \approx g$. The shear describes the change in the observed ellipticity of a galaxy, ϵ^s, as:

$$\epsilon = \epsilon^s + \gamma\,. \tag{1.6}$$

The value of the shear can be estimated by averaging a large number of observed ellipticities, if galaxies are randomly oriented, as $\langle\epsilon\rangle = \gamma$. This means that gravitational lensing produces an apparent alignment of galaxy shapes. However, gravitational tidal forces can induce a distortion in the shape of galaxies that can produce an *intrinsic* alignment, which can be a non-negligible fraction of the *apparent* alignment induced by gravitational lensing. The intrinsic alignment can be important for all types of weak lensing analyses, since by its very nature the effect of weak lensing is too small to be detected using the shape of a single galaxy, and so it must be studied statistically. The need for a statistical study to obtain the weak lensing signal is at the very heart of why the intrinsic alignment of galaxies can be a source of nuisance for weak lensing studies.

Galaxy intrinsic and apparent alignments

Even if GL can be expressed in its simpler form as the effect of a single source on a single light ray, in reality the Universe is filled with light and matter. Nearly all of the light emitted by distant galaxies could be influenced by intervening matter, enabling the study of the matter distribution of the Universe. Moreover, by dividing sources in redshift, and by studying the distortion induced by gravitational lensing on their images, is possible to probe how the distribution of matter changes throughout cosmic time, providing us with the opportunity to constrain the cosmological parameters of the Universe. This application of weak lensing is called *cosmic shear*. In practice, cosmic shear connects the lensing power spectrum to the matter power spectrum, by measuring the galaxy shapes correlations induced by GL (see Kaiser 1992; Bartelmann & Schneider 2001; Schneider 2005; Hoekstra & Jain 2008, for reviews on the applications of weak lensing to constrain cosmological parameters).

Here we will not go into the details of cosmic shear, but instead highlight one of the main complications for the cosmic shear measurements: the intrinsic alignment.

Cosmic shear measurements are obtained in the form of projected 2-point correlation functions (or their equivalent angular power spectra) between galaxy shapes.

$$\langle\epsilon\epsilon\rangle = \langle\gamma\gamma\rangle + \langle\gamma\epsilon^s\rangle + \langle\epsilon^s\gamma\rangle + \langle\epsilon^s\epsilon^s\rangle \tag{1.7}$$

$$= GG + GI + IG + II\,. \tag{1.8}$$

If we assume that galaxies are not intrinsically oriented towards one another, then the only correlations in the shape and orientation of observed galaxies are due to the gravitational lensing effect of the intervening mass distribution between the sources and the observer, $\langle\gamma\gamma\rangle$.

Here the only nonzero term is the GG (shear-shear) auto correlation. In the case of a non-negligible intrinsic alignment of galaxies, the second term is also nonzero, i.e. part of the correlation between the shape and orientation of galaxies is *intrinsic*. If the same gravitational forces that shear the light emitted from a galaxy also tidally influence the intrinsic shape of other galaxies, then this will produce a nonzero cross-correlation between shear and intrinsic shape (GI). The term IG is zero since a foreground galaxy cannot be lensed by the same structure that is tidally influencing a background galaxy, unless their respective positions along the line of sight is confused due to large errors in the redshift measurements. In **Chapter 4** we study the *intrinsic* alignment of galaxies in hydrodynamical cosmological simulations.

Most intrinsic alignment theories predict the alignment of dark matter structures. On the other hand, the alignment of galaxies is measured using the light of galaxies, and so it is often assumed that the light traces dark matter, or alternatively that the misalignment between haloes and galaxies is known. The misalignment between galaxies and their haloes is studied in **Chapter 3** using hydrodynamical cosmological simulations.

Galaxy-galaxy lensing

The shear is measured with respect to the projected separation vector of the source-lens pair: the tangential shear, $\gamma_{\rm t}$, defined as

$$\gamma_t = \gamma \cos(2\Phi), \tag{1.9}$$

where Φ is the position angle.

One of the advantages of measuring the tangential shear is that it is directly related to the excess surface mass density (ESD)

$$\gamma_{\rm t}(r_{\rm p}) = \frac{\Delta\Sigma(r_{\rm p})}{\Sigma_{\rm cr}}, \tag{1.10}$$

that in turn relates to the surface density as

$$\Delta\Sigma(r_{\rm p}) \equiv \bar{\Sigma}(< r_{\rm p}) - \Sigma(r_{\rm p}), \tag{1.11}$$

where $r_{\rm p}$ is the projected distance from the centre of the halo, $\bar{\Sigma}(< r_{\rm p})$ is the surface density within $r_{\rm p}$ and $\Sigma(r_{\rm p})$ is the surface density at $r_{\rm p}$. By stacking the shear signal in concentric rings, the radial profile of the ESD can be studied. Galaxy-galaxy weak lensing (GGL) is the study of the ESD profile of galaxies measured through staking the shear signal of background galaxies around the position of lenses. Since the shear of a single lens system is usually too small to be detected, the properties of individual galaxies can not be constrained with GGL. Instead, if the lenses are chosen according to a given property, for example the stellar mass, the statistical property of a selected population of lens galaxies can be studied. In recent years, galaxy-galaxy weak lensing has become a viable way to statistically constrain the mass, density profiles and ellipticity of the dark matter haloes. In **Chapter 5** we compare the ESD from simulations with the galaxy-galaxy lensing signal observed using background galaxies imaged by the KiDS survey around spectroscopically confirmed foreground galaxies from the GAMA survey.

Another application of galaxy-galaxy lensing is the measure of the average shape of haloes. For this application, in the stacking process the lens galaxies are re-oriented according to the direction of the major axis of their light distribution. In this way, for a triaxial halo the value of the tangential shear along the major and minor axes of the galaxy is expected to be different. It is possible to translate this difference into a constraint on the halo shape of galaxies. The halo shapes represent an interesting line of study because they are expected to be triaxial in the ΛCDM framework and spherical in some alternative cosmology theories. Of course, the main assumption of these studies is that the major axis of light distribution aligns with the major axis of the halo. Therefore, the shape measurement can be affected by the presence of a misalignment between the galaxy and the dark matter halo.

1.3 This Thesis

Our first step in exploring the connection between baryons and their host haloes is to study how the inclusion of baryonic physics can alter the properties of haloes in a cosmological simulation. Along these lines, in **Chapter 2** we study the effect of baryon physics on the masses and profiles of haloes and consequently on their abundance in a unit volume (known as the halo mass function). We find that gas expulsion and the associated dark matter (DM) expansion induced by supernova-driven winds are important for haloes with masses $M_{200} \leq 10^{13}\,\mathrm{M}_{\odot}$, lowering their masses by up to 20% relative to a DM-only model. AGN feedback has a significant impact on halo masses up to cluster scales ($M_{200} \sim 10^{15}\,\mathrm{M}_{\odot}$). Baryon physics changes the total mass profiles of haloes out to several times the virial radius, a modification that can only capture by changing the the functional forms used to commonly fit halo profiles. The decrease in the total halo mass causes a decrease in the halo mass function of about 20%. The analysis presented in **Chapter 2** indicates that baryonic processes can significantly alter the properties of dark matter haloes. Therefore, their inclusion is essential in simulations aiming to give theoretical support to observations that are probing the total mass of haloes.

Gravitational lensing offers a way to detect dark matter haloes in observations. In this context, hydrodynamical cosmological simulations serve as a tool to study and mitigate possible shortcomings of gravitational lensing. In **Chapter 3** we make use of four hydrodynamical simulations, run in increasingly larger volumes and covering over four orders of magnitude in mass ($11 \leq \log_{10}(M_{200}/[\,h^{-1}\,\mathrm{M}_{\odot}]) \leq 15$), to study the misalignment between galaxies and their host haloes as a function of radius and redshift. The galaxy-halo misalignment has profound implications for gravitational lensing studies that aim to constrain the shape of dark matter haloes, since lens galaxies are stacked according to the direction of their major axis under the assumption that it aligns with the major axis of the halo. The shape of the halo is constrained by examining the different shear signals along the major and the minor axes of the stacked galaxies. Therefore, the shape measurement can be affected by the presence of a misalignment between the galaxy and the dark matter halo for which the shape is measured. Moreover, the misalignment between galaxies and their haloes also represents a relevant field of study for the intrinsic alignment. In fact, most intrinsic alignment theories predict the alignment of dark matter structures and thus, in order to be tied to the observations, the misalignment between haloes and galaxies must be known. In our study, we found that galaxies align well with the local distribution of the total (but mostly dark) matter, however, the stellar distributions on galactic scales exhibit a significant misalignment with respect to their host haloes. This misalignment is reduced in the most massive haloes. This implies that the orientation of galaxies is a good tracer of the dark matter, only on comparable scales. On larger scales, a significant misalignment exists between galaxies and their haloes, which must be accounted for in weak lensing studies.

Another potential contaminant of weak gravitational lensing measurements is the alignment of galaxies between themselves, known as intrinsic galaxy alignment. In fact, in the limit of a very weak lensing signal, the distortion induced via gravitational forces (giving rise to an *intrinsic* alignment) can be a non-negligible fraction of the distortion due to the pure gravitational lensing effect (often termed *apparent* alignment). In **Chapter 4** we report results for the *intrinsic* alignment of galaxies in hydrodynamical cosmological simulations. Specifically, we focus on the orientation-direction, which is the angle between the major axis and the direction of a nearby galaxy, and the orientation-orientation alignment, which is the angle between the major axes of nearby galaxies. We find that while the strength of the alignment is a strongly decreasing function of the distance between galaxies, it can remain significant up to $\sim$ 100 Mpc, with more massive haloes demonstrating stronger alignment. We find a significant decrease in the alignment of galaxies when orientations are computed using only stars within the typical observable extent of a galaxy rather than using all stars associated with the subhalo. This difference may account for the common findings reported in the literature of galaxy alignments being systematically stronger in simulations than in observations. Particular care must be taken in the sample of stars that are considered, since this can ultimately result in very different alignment strengths. The orientation-orientation alignment is always weaker than the orientation-direction alignment, which suggests that galaxy alignment is driven by the position of nearby haloes, whereas the mutual orientations of nearby galaxies is a consequence of this effect.

Through galaxy-galaxy lensing, it is possible to directly measure the mass and mass profiles of haloes as well as the connection between the stellar and halo masses of galaxies. In **Chapter 5** we report the study of the galaxy-galaxy lensing signal for galaxies in the EAGLE simulations divided into six stellar mass bins. We compare the results from the simulations to the observed signal, which was measured using background galaxies imaged by the KiDS survey around spectroscopically confirmed foreground galaxies from the GAMA survey. The GAMA group catalogue offers us the possibility to compare the central and satellite contribution to the total signal separately. Overall, the predicted lensing signal is in broad agreement with the observations, as expected due to the fact that the EAGLE simulation has been calibrated to reproduce the observed $z \sim 0$ galaxy stellar mass function. We find good agreement between the data and predictions from EAGLE for both central and satellite galaxies. When satellite and central galaxies are analyzed jointly, the agreement worsens. This stems from the fact that the total GGL profile is a linear combination of central and satellite profiles with the satellite fraction as the linear coefficient, and the satellite fraction in the EAGLE simulation is always lower than that of the GAMA group catalogue.

Bibliography

Bartelmann, M., & Schneider, P. 2001, Phys. Rep., 340, 291

Crain, R. A., Schaye, J., Bower, R. G., et al. 2015, MNRAS, 450, 1937

Frenk, C. S., & White, S. D. M. 2012, Annalen der Physik, 524, 507

Hoekstra, H., & Jain, B. 2008, Annual Review of Nuclear and Particle Science, 58, 99

Kaiser, N. 1992, ApJ, 388, 272

Le Brun, A. M. C., McCarthy, I. G., Schaye, J., & Ponman, T. J. 2014, MNRAS, 441, 1270

McCarthy, I. G., Le Brun, A. M. C., Schaye, J., & Holder, G. P. 2014, MNRAS, 440, 3645

Schaye, J., Dalla Vecchia, C., Booth, C. M., et al. 2010, MNRAS, 402, 1536

Schaye, J., Crain, R. A., Bower, R. G., et al. 2015, MNRAS, 446, 521

Schneider, P. 2005, ArXiv Astrophysics e-prints, astro-ph/0509252

Springel, V. 2010, ARA&A, 48, 391